

Analysis of perturbed magnetic fields via construction of nearby integrable fields

S. R. Hudson^{a)}

Plasma Theory Laboratory, Japan Atomic Energy Research Institute, Naka-gun, Ibaraki-ken, Japan

R. L. Dewar

Dept. of Theoretical Physics & Plasma Research Laboratory, R.S.Phys.S.E., Australian National University, A.C.T., 0200, Australia

(Received 26 October 1998; accepted 22 January 1999)

For a given nonintegrable toroidal magnetic field, a nearby integrable magnetic field is constructed from quadratic-flux minimizing surfaces. A new mathematical definition and derivation of quadratic-flux minimizing surfaces, which directly exploits the analogy between toroidal magnetic fields and $1\frac{1}{2}$ degree of freedom Hamiltonian systems, is given. The width and phase of magnetic islands (calculated from the shear of the integrable field and the magnitude and phase of the perturbation harmonics) are in excellent agreement with detailed Poincaré plots. © 1999 American Institute of Physics. [S1070-664X(99)01305-1]

I. INTRODUCTION

Many treatments of magnetic field configurations, plasma dynamics and general Hamiltonian systems, utilize the assumption of a nearby, integrable system to which the actual system is considered as a small perturbation.¹ In Hamiltonian systems, for example,² often the analytic form of the nearby integrable Hamiltonian is known. Standard perturbation theory constructs action-angle coordinates for the integrable system and the Fourier harmonics of the perturbation can be used to determine resonance widths.

Since toroidal magnetic fields used for the containment of plasmas are analogous to $1\frac{1}{2}$ dimensional Hamiltonian systems,³ the same ideas are appropriate for understanding magnetic field structure. In fact, the assumption that the magnetic field is integrable, or at least that the magnetic field is nearby an integrable field, is widespread in theoretical research in many areas of tokamaks and stellarator physics. This is partly because good flux surfaces improve plasma confinement, and thus the existence of flux surfaces is essential for any magnetic configuration relevant for the containment of fusion plasmas; and partly because the coordinate systems that integrable fields allow, namely flux coordinates or straight field line coordinates, aid the researcher to see past the geometrical complexity of plasma confinement devices and concentrate on the physical issues. The importance of flux coordinates for example, is evidenced by the widespread usage of Boozer coordinates⁴ in which the magnetic field and the equations governing the plasma take a particularly simple form. At the heart of plasma analysis based on flux coordinates is the assumption that an integrable magnetic field exists, or more generally that the actual magnetic

field may be considered to be a small perturbation to an integrable field.

However, for complicated magnetic confinement systems the nearby integrable field is not known initially. Furthermore, to any given nearby integrable field, there is any number of integrable fields which are nearby: the term “nearby” is not uniquely defined. Any set of toroidal surfaces may be used to construct an integrable field. The question then arises: which set of surfaces is most useful for constructing the preferred nearby integrable field?

Previous treatments of this problem have utilized the flux surfaces surviving perturbation of the given nonintegrable magnetic field, which are called the KAM surfaces, and have assigned straight-field-line coordinates to these surfaces. One approach locates good flux surfaces by following field lines.⁵ The field lines that lie on closed flux surfaces are assigned to be straight-field-lines of a nearby integrable magnetic field. Important research in this field was presented by Boozer, who showed how to determine a convenient representation for integrable magnetic fields by field line tracing⁴ and gave a useful representation of a general magnetic field.⁶ Another technique⁷ utilizes a generating function and minimizes the variation of an integrable Hamiltonian over a trial torus with respect to the parameters defining the Hamiltonian.

Such methods are convenient for some applications, because they guarantee that the constructed integrable field coincides with the original field on the flux surfaces and thus allow straight-field-line coordinates for the original magnetic field to be constructed in regions of good flux surfaces. However, using KAM surfaces of the nonintegrable field to define a nearby integrable field has the unfortunate consequence that the integrable field becomes singular at the separatrices. Also, when a field line is chosen, it is not known whether that field line will lie on a good flux surface, or whether it is a chaotic field line or lies within an island chain.⁸ Problems

^{a)}Present address: University of Wisconsin, 1500 Engineering Drive ERB511, Madison, WI 53706; Electronic mail: hudson@cptc.wisc.edu

with field line tracing methods may arise near low order rational surfaces.⁵

Recently, an approach has been developed which uses surfaces that pass directly through the resonances of any chosen island chain to construct an integrable magnetic field. The surfaces are defined as those surfaces which extremize a deviation from invariance, and are called quadratic-flux minimizing surfaces. This article will revise and extend work presented in several earlier papers^{9,10} in a complete and mathematically simple manner. In this paper, we present a revised construction of quadratic-flux minimizing surfaces which utilizes the magnetic field line action. Though this approach seems somewhat abstract, the subsequent analysis is simpler than the original presentation and sheds more insight into the analogy between Hamiltonian systems and magnetic field line flow. The quadratic-flux minimizing surfaces constructed are considered as replacement flux surfaces for nonintegrable fields and are used to define a nearby integrable magnetic field for which straight field line coordinates may be constructed. In this article, the previous analysis has been extended to calculate the magnitude of resonant perturbation harmonics. This information, along with the shear of the constructed integrable system, is used to accurately calculate island widths. Comparison of the calculated island widths with detailed Poincaré plots show very good agreement.

In Sec. II, we review a convenient representation of the magnetic field in arbitrary toroidal coordinates and discuss some desirable features of a suitable nearby integrable field and a Hamiltonian perspective of flux surfaces. In Sec. III, we derive quadratic-flux minimizing surfaces from an analogy with Hamiltonian concepts and outline their construction. A radial coordinate is introduced with level surfaces that coincide with the quadratic-flux minimizing surfaces. In Sec. IV, an angle coordinate is used to complement the radial coordinate and implicitly define a nearby integrable magnetic field. The perturbation terms are used to derive estimates for the island widths which are compared to Poincaré plots obtained using the Princeton iterative equilibrium solver (PIES) code in Sec. V.

II. REPRESENTATION OF THE MAGNETIC FIELD

Any coordinate system may be used to represent the magnetic field. For toroidal magnetic fields, Cartesian, cylindrical, or toroidal coordinate systems may be used. Each may have advantages or disadvantages depending on the particular application. We assume here that the magnetic field is expressed in arbitrary toroidal coordinates (ρ, θ, ϕ) , and we assume stellarator symmetry which enables the magnetic field to be expressed :

$$B^\rho = \sum_{n,m} B_{n,m}^\rho(\rho) \sin(n\theta - m\phi), \tag{1}$$

$$B^\theta = \sum_{n,m} B_{n,m}^\theta(\rho) \cos(n\theta - m\phi), \tag{2}$$

$$B^\phi = \sum_{n,m} B_{n,m}^\phi(\rho) \cos(n\theta - m\phi). \tag{3}$$

The transformation to cylindrical coordinates (R, ϕ, z) is

$$R = R_{\text{maj}} + \sum_{n,m} x_{n,m}(\rho) \cos(n\theta - m\phi),$$

$$z = \sum_{n,m} y_{n,m}(\rho) \sin(n\theta - m\phi). \tag{4}$$

The Jacobian of the (ρ, θ, ϕ) coordinates, $\mathcal{J}_{\rho\theta\phi}$, is given by $\mathcal{J}_{\rho\theta\phi} = (\partial_\theta R \partial_\rho z - \partial_\rho R \partial_\theta z) R$. The toroidal angle ϕ is chosen to coincide with the usual cylindrical angle for later convenience.

An integrable field is defined implicitly by a set of straight-field-line coordinates.¹¹ The typical starting assumption required for the existence of straight-field-line coordinates is the assumption that all field lines lie on nested toroidal flux surfaces. As the existence of such surfaces is not necessarily the case everywhere for a general magnetic field, the first step is to construct a set of ‘‘replacement’’ surfaces which may be identified as flux surfaces of some integrable field. The second step is to introduce a suitable straight-field-line angle coordinate to complement the surfaces and complete the coordinate system. We discuss these two steps separately.

First we construct a set of toroidal surfaces. There are some properties that we wish our construction of surfaces to satisfy. The typical perturbation analysis approach assumes an integrable field for which straight-field-line coordinates are constructed, and then a small perturbation is added. Following this construction, we note that both the X and O points of any particular island chain will lie on the same flux surface of the integrable field—that particular flux surface with the rotational transform appropriate for the periodicity of the X and O orbits. Thus we require that the surface to be used as a flux surface of the integrable field pass through both the X and O points of chosen island chains. The rotational transform of this surface must also be exactly that of the island chain (a rational), and the X and O trajectories of the perturbed magnetic field should coincide with periodic trajectories of the constructed integrable field. Perturbation theory generally requires the perturbation terms to be small. Thus we prefer an integrable field that is ‘‘as close as possible’’ to the given field. Here, as close as possible is interpreted as requiring that the Fourier representation of the perturbation field is minimal. Also, in the trivial case where we begin with an integrable field, the construction of the replacement surfaces should reduce simply to the original flux surfaces. We require a computationally efficient algorithm for constructing the surfaces in a way which is physically insightful. To be useful in analyzing magnetic configurations the algorithm must be robust and flexible. Finally, we note that even though the nonintegrable field may contain some flux surfaces, those flux surfaces will generally not coincide with the flux surfaces of the underlying integrable field. That is, the flux surfaces of the underlying integrable field are deformed by perturbation. In the following analysis, we will not impose the constraint that the flux surfaces of the nearby integrable field must coincide with the flux surfaces surviving perturbation of the given nonintegrable field; nevertheless, as shown in Sec. V, we may choose this to be the case

and construct an integrable field which with flux surfaces that coincide with the chosen flux surfaces of the given non-integrable field. This can be convenient for constructing straight-field-line coordinates for nonintegrable magnetic fields in regions of good flux surfaces.

We approach the problem of defining and constructing a set of replacement surfaces by reviewing the concept of flux surfaces. Using the terminology of plasma confinement physics, flux surfaces may be defined as toroidal surfaces on which the magnetic field is everywhere tangential—that is $B^n = \mathbf{B} \cdot \mathbf{n} = 0$ on the flux surface, where \mathbf{n} is the normal to the surface. Equivalently, we may define flux surfaces as those surfaces for which the following surface integral is zero:

$$\varphi_2 = \frac{1}{2} \int (B^n)^2 d\sigma = 0. \tag{5}$$

Rather than consider surfaces that set this integral to zero, which is not always possible in all regions of space for a general magnetic field, we consider the surfaces that extremize a similar functional. In this article, we depart from the previous analysis⁹ to develop a clearer definition and construction of quadratic-flux minimizing surfaces.

The simplest definition and analysis uses the methods of Hamiltonian dynamical systems, which we briefly review. The analog of the Lagrangian in noncanonical coordinates (ρ, θ, ζ) is the magnetic vector potential and the action along a closed trial curve is written³

$$S = \oint \mathbf{A} \cdot d\mathbf{l} = \oint (A_\rho \dot{\rho} + A_\theta \dot{\theta} + A_\zeta \dot{\zeta}) d\zeta, \tag{6}$$

where the dot represents derivative with respect to ζ , and ζ is chosen to parameterize position along a field line. Here we use ζ to represent the arbitrary toroidal angle coordinate to reflect the fact that the theory is valid in general toroidal coordinates. For arbitrary variations $\delta\rho(\zeta), \delta\theta(\zeta)$ the variation in the action may be written

$$\delta S = \oint \left(\frac{\delta S}{\delta\rho} \delta\rho + \frac{\delta S}{\delta\theta} \delta\theta \right) d\zeta, \tag{7}$$

with the Fréchet derivatives being

$$\frac{\delta S}{\delta\rho} = \mathcal{J}(B^\zeta \dot{\theta} - B^\theta), \quad \frac{\delta S}{\delta\theta} = \mathcal{J}(B^\rho - B^\zeta \dot{\rho}). \tag{8}$$

Hamilton's principle² states that the dynamics extremizes the action integral and the Euler–Lagrange equations are obtained by setting each of the Fréchet derivatives to zero: $\dot{\theta} = B^\theta/B^\zeta, \dot{\rho} = B^\rho/B^\zeta$.

In the integrable limit, there exist irrational rotational-transform surfaces and rational rotational-transform surfaces. Each irrational rotational-transform surface is covered densely by a single magnetic field line. Depending on the ‘‘irrationality’’ of the rotational-transform and the magnitude of the perturbation, the irrational flux surfaces may survive perturbation, though they will generally be slightly deformed. These surfaces are referred to as the KAM surfaces.¹² Each rational rotational-transform surface is comprised of a family of periodic magnetic field lines which are degenerate in action and along which the action gradients

$\delta S/\delta\theta$ and $\delta S/\delta\rho$ are zero. Rational surfaces are destroyed by perturbation and islands form. Typically, two periodic orbits survive perturbation and are referred to as the X and O points.

III. QUADRATIC-FLUX MINIMIZING SURFACES

For typical nonintegrable systems, we cannot generally expect that a surface may be found on which $\delta S/\delta\theta$ and $\delta S/\delta\rho$ are both zero everywhere, so a more general variational principle is required. In this section, we introduce quadratic-flux minimizing surfaces as surfaces that extremize a natural extension of Eq. (5), the quadratic-flux functional, which we define in analogy with Lagrangian dynamics and derive the Euler-Lagrange equation for extremal surfaces.

To obtain the quadratic-flux functional, the first of the action gradients, $\delta S/\delta\rho$, is set equal to zero as a constraint: $\delta S/\delta\rho = 0$. This enables the use of the equation $\dot{\theta} = B^\theta/B^\zeta$. The other term, $\delta S/\delta\theta$, shall be minimized over a toroidal surface defined by $\rho = P(\theta, \zeta)$ by considering the quadratic-flux functional, or in this case the square of the action gradient functional $(\delta S/\delta\theta)^2$

$$\varphi_2 = \frac{1}{2} \int \int \left[\frac{\delta S}{\delta\theta} \right]^2 d\theta d\zeta. \tag{9}$$

The trial surface $\rho = P(\theta, \zeta)$ is varied by δP , and the corresponding variation in φ is evaluated

$$\delta\varphi = \int_0^{2\pi} \int_0^{2\pi} [\delta(\mathcal{J}B^\rho) - \delta\dot{\rho}(\mathcal{J}B^\zeta) - \dot{\rho}\delta(\mathcal{J}B^\zeta)] \frac{\delta S}{\delta\theta} d\theta d\zeta. \tag{10}$$

The term $\delta\dot{\rho}$ is written

$$\delta\dot{\rho} = \frac{\partial_\rho B^\theta \delta P \partial_\theta P}{B^\zeta} - \frac{B^\theta \partial_\rho B^\zeta \delta P \partial_\theta P}{(B^\zeta)^2} + \frac{B^\theta \partial_\theta \delta P}{B^\zeta} + \partial_\zeta \delta P. \tag{11}$$

Substituting this form into Eq. (10), integrating the terms involving $\partial_\theta \delta P$ and $\partial_\zeta \delta P$ by parts and noting that for an arbitrary function f

$$\partial_\theta (\mathcal{J}B^\theta f) = \partial_\theta (\mathcal{J}B^\theta) f + \partial_\rho (\mathcal{J}B^\theta) \partial_\theta P f + (\mathcal{J}B^\theta) \partial_\theta f, \tag{12}$$

we obtain

$$\delta\varphi_2 = \int_0^{2\pi} \int_0^{2\pi} \delta P (B^\theta \partial_\theta + B^\zeta \partial_\zeta) \frac{\delta S}{\delta\theta} d\theta d\zeta. \tag{13}$$

On setting the first variation $\delta\varphi_2$ to zero we obtain the Euler–Lagrange equation for extremizing surfaces which we call quadratic-flux minimizing surfaces:

$$(B^\theta \partial_\theta + B^\zeta \partial_\zeta) \frac{\delta S}{\delta\theta} = 0. \tag{14}$$

The Euler–Lagrange equation indicates the action gradient, $\delta S/\delta\theta$, is constant along the tangential dynamics defined on the surface. We identify and define the pseudofield as the field associated with the tangential dynamics

$$\mathbf{B}_\nu \cdot \nabla = (B^\theta \partial_\theta + B^\zeta \partial_\zeta). \tag{15}$$

The above analysis was originally presented using the terminology of magnetic field line flows. We restate the two main equations for completeness. The quadratic-flux functional may be written

$$\varphi_2 = \frac{1}{2} \int_{\Gamma} \frac{B_n^2}{C_n} d\sigma, \tag{16}$$

with $B_n = \mathbf{B} \cdot \mathbf{n}$ and $C_n = \nabla \theta \times \nabla \zeta \cdot \mathbf{n}$ for \mathbf{n} unit normal to the surface Γ . The Euler–Lagrange equation resulting from Eq. (16) is⁹

$$\mathbf{B}_\nu \cdot \nabla \nu = 0, \tag{17}$$

where $\mathbf{B}_\nu \equiv \mathbf{B} - \nu \mathbf{C}$ and $\nu \equiv B_n / C_n$. We call \mathbf{B}_ν the pseudofield and observe that ν is equal to the action gradient, $\nu \equiv \partial S / \partial \theta$.¹³

The Euler-Lagrange equation Eq. (14) indicates that a rational rotational-transform quadratic-flux minimizing surface is comprised of a family of periodic pseudo-orbits. We define pseudo-orbit as an integral curve of the pseudomagnetic field. Along each periodic pseudo-orbit that lies on a quadratic-flux minimizing surface, the action gradient remains constant. Each periodic pseudo-orbit closes upon itself after an appropriate number of toroidal and poloidal transits, and is located via a two-dimensional search in (ρ, θ) . The details of a slight variant of this approach for the construction of quadratic-flux minimizing surfaces and a discussion of the action gradient parameter is presented in Ref. 10.

Dewar *et al.*⁹ showed that rational rotational-transform quadratic-flux minimizing surfaces pass directly through the resonances, and both X and O points of any given island chain lie on the same quadratic-flux minimizing surface. Also, in regions where the magnetic field lines lie on flux surfaces, the quadratic-flux minimizing surfaces will coincide with the flux surfaces. This ensures that if we apply our construction of a nearby integrable field to an actual integrable field, then we will simply obtain the original field.

Returning to the topic of construction of an integrable magnetic field nearby a given nonintegrable magnetic field, we may construct a set of rational quadratic-flux minimizing surfaces. Any quadratic-flux minimizing surface may be chosen, provided the rotational-transform of the surface is within the range defined by the rotational-transform profile of the nonintegrable magnetic field. The selection of surfaces is somewhat arbitrary, but important since the choice of surfaces greatly effects the resultant integrable magnetic field as will be shown in Sec. V. The quadratic-flux minimizing surfaces are identified as flux surfaces of a nearby integrable field.

IV. STRAIGHT-FIELD-LINE ANGLE

It remains to introduce an appropriate angle coordinate to complete the set of coordinates which will define a nearby integrable field. As an intermediate step in the construction, we perform a vector transformation to coordinates using the quadratic-flux minimizing surfaces as the level surfaces of the radial coordinate at a discrete set of values. An interpolation provides a smooth continuous radial coordinate, which

we label with s . After performing a coordinate transformation to coordinates (s, θ, ζ) , we may write the magnetic field

$$\mathbf{B} = B^s \mathbf{e}_s + B^\theta \mathbf{e}_\theta + B^\phi \mathbf{e}_\phi. \tag{18}$$

This form is useful as the components of the magnetic field that destroy integrability are recognized as the function $B^s(s, \theta, \phi)$. We construct the integrable field from the original nonintegrable field by subtracting the terms which destroy the integrability. These are directly related to the action gradient terms, which are exactly the quantities minimized by the quadratic-flux minimization procedure. We thus conclude that this approach gives a clear definition of the term as close as possible.

We obtain the preferred angle coordinate by constructing an integrable field. An integrable magnetic field, $\bar{\mathbf{B}}$, with invariant surfaces coinciding with the tori $s = const$, would have $\bar{B}^s \equiv 0$. We construct such a field from \mathbf{B} by seeking a divergence-free correction field, $\delta \mathbf{B}$, such that $\mathcal{J}_{s\theta\phi} \delta B^s = -\nu$, where we now use ν to represent $\mathcal{J}_{s\theta\phi} B^s$. If we can find such a field, then the total field $\bar{\mathbf{B}} \equiv \mathbf{B} + \delta \mathbf{B}$ will automatically satisfy the integrability condition $\mathcal{J}_{s\theta\phi} \bar{B}^s \equiv 0$. An equation for $\delta \mathbf{B}$ is provided by the divergence-free condition

$$\partial_\theta (\mathcal{J}_{s\theta\phi} \delta B^\theta) + \partial_\phi (\mathcal{J}_{s\theta\phi} \delta B^\phi) = \partial_s \nu. \tag{19}$$

This may be solved using the Fourier components of the magnetic field:¹⁰

$$\begin{aligned} & ((\mathcal{J}_{s\theta\phi} \delta B^\theta)_{nm}, (\mathcal{J}_{s\theta\phi} \delta B^\phi)_{nm}) \\ &= \begin{cases} (0, 0), & n=0, m=0 \\ (\partial_s \nu_{n,m}/m, 0), & n=0, m \neq 0 \\ (0, -\partial_s \nu_{n,m}/n), & n \neq 0, m=0 \\ (\partial_s \nu_{n,m}/m, 0), & n \neq 0, m \neq 0 \end{cases} \end{aligned} \tag{20}$$

By adding these correction terms to the original nonintegrable magnetic field we obtain an integrable magnetic field for which we may construct straight field line coordinates [Ref. 11, pp. 116–120], which we label (s, θ_0, ϕ) . The original magnetic field \mathbf{B} is written in the (s, θ_0, ϕ) coordinates by a standard vector transformation and the new Jacobian $\mathcal{J}_{s\theta_0\phi} = \mathcal{J}_{s\theta\phi} \partial \theta_0 / \partial \theta$ is obtained.

Continuing on from the previous work, we note that the coordinates thus constructed enable the original magnetic field to be expressed in terms of a canonical nearby integrable field-line Hamiltonian, χ , such that

$$\mathbf{B} = \nabla \psi_t(s) \times \nabla \theta_0 + \nabla \phi \times \nabla \chi(s, \theta_0, \phi), \tag{21}$$

where $\chi = \chi_0(s) + \sum_{nm} \chi_{nm}(s) \cos(n\phi - m\theta_0)$. The Fourier components of the magnetic field in (s, θ_0, ϕ) coordinates are simply related to the Fourier components of the field line Hamiltonian through

$$(\mathcal{J}_{s\theta_0\phi} B^s)_{nm} = -m \chi_{nm}, \quad (\mathcal{J}_{s\theta_0\phi} B^{\theta_0})_{nm} = \dot{\chi}_{nm}. \tag{22}$$

It is convenient to use the field line Hamiltonian representation, as this algebraic form guarantees the divergence-free property of the magnetic field. The field line Hamiltonian provides all information regarding the magnetic field.

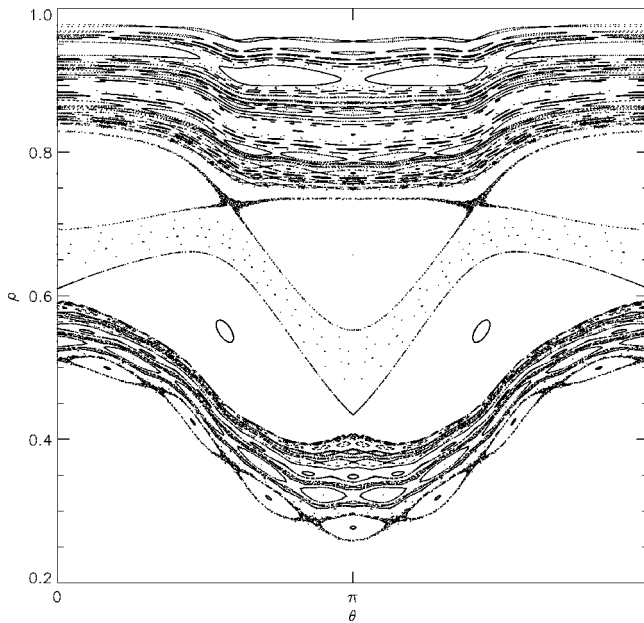


FIG. 1. Poincaré plot in background coordinates (ρ, θ, ϕ) .

The perturbation components, χ_{nm} , of the original field are easily identified as the difference between the integrable field and the original field. The χ_{nm} can be used to determine accurate estimations of the (n, m) island width as follows. Consider for example the Hamiltonian with a single resonance $\chi = \chi_0(s) - \chi_{nm}(s)\cos(n\phi - m\theta)$. Using the generating function $F_2 = (n\phi - m\theta_0)\hat{s}$ we transform to rotating coordinates and obtain the transformed Hamiltonian $\hat{\chi} = \chi_0(s) - \chi_{nm}(s)\cos(\hat{\theta}_0) - ns/m$. The periodic orbits are located at $\hat{\theta}_0 = 0, \pi$. Which orbit is stable or unstable depends on both the sign of the integrable shear ι^{-1} , where $\iota = \chi'_0$, and the sign of χ_{nm} . For now, we assume the unstable periodic orbit corresponds to $\hat{\theta}_0 = \pi$. To determine the island width, we must find the solutions s_{\pm} to

$$\chi_0(s_{\pm}) - \chi_{nm}(s_{\pm}) - \frac{ns_{\pm}}{m} = \chi_0(s_{nm}) + \chi_{nm}(s_{nm}) - \frac{ns_{nm}}{m}. \tag{23}$$

There will be two solutions, s_+ and s_- , corresponding to the upper branch of the separatrix and the other to the lower branch respectively, which may be found numerically. In the small-island approximation, the variation in χ_{nm} across the island is assumed negligible, and an expansion is made to obtain the usual formula. $\Delta s = \pm 2\sqrt{\chi_{nm}/\iota'}$.

V. RESULTS

For an example, we use a magnetic field consistent with the tokamak JT60-U reversed shear parameters calculated using the PIES¹⁴ code. A profile is used with $q_{\min} < 2$, so two $q=2$ rational surfaces are present. A Poincaré plot Fig. 1 shows two large $q=2$ island chains, as well as higher order island chains and small regions of chaos. This configuration was chosen because it is currently an important research topic at Japan Atomic Energy Research Institute (JAERI).^{15,16}

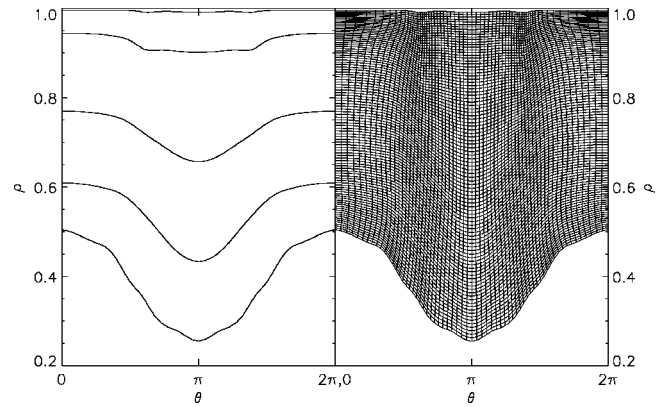


FIG. 2. (a) (left) A cross section of the quadratic-flux minimizing surfaces chosen for radial framework, on the toroidal plane $\phi=0$. (b) (right) The resulting coordinate grid.

Using the same magnetic field, we will show two example cases chosen to illustrate some features of the procedure. First we will construct a nearby integrable field that may be understood as an underlying integrable field to which the given nonintegrable magnetic field may be considered as a small perturbation. Second, we construct an integrable field with flux surfaces that coincide with flux surfaces of the given nonintegrable field. The different outcomes is determined by the initial choice of quadratic-flux minimizing surfaces.

To display the first construction, we choose a set of quadratic-flux minimizing surfaces that will form the framework of the new radial coordinate. We choose surfaces that pass through the lowest order island chains, namely the two $q=2$ surfaces and the $q=3$ surface. Two other surfaces are required to define the boundary of the interpolation region. The surfaces chosen and the constructed coordinate grid are shown in Fig. 2.

The Fourier components of the perturbation with $(n, m) = (2, 1), (3, 1)$, and the q profile are shown in Fig. 3(a). Shown in Fig. 3(b) is a Poincaré plot of the same magnetic

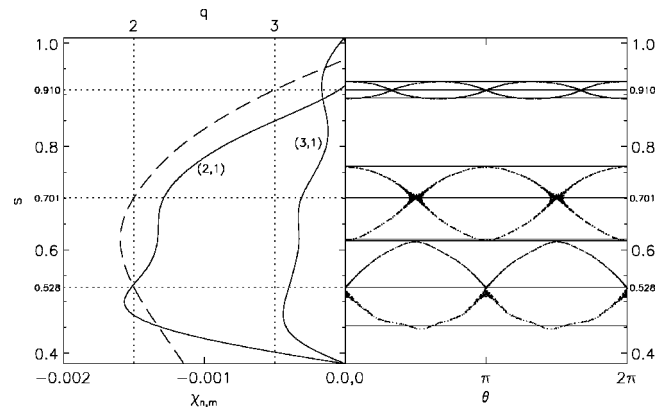


FIG. 3. (a) (left) Resonant perturbations with $(n, m) = (2, 1), (3, 1)$ shown with solid lines, and the q profile shown with dashed line. (b) (right) The Poincaré plot in new coordinates showing $(n, m) = (2, 1), (3, 1)$ island chains with the $(2, 1)$ and $(3, 1)$ rational surfaces and estimated island widths plotted as solid horizontal lines. The coordinates correspond to those shown in Fig. 2.

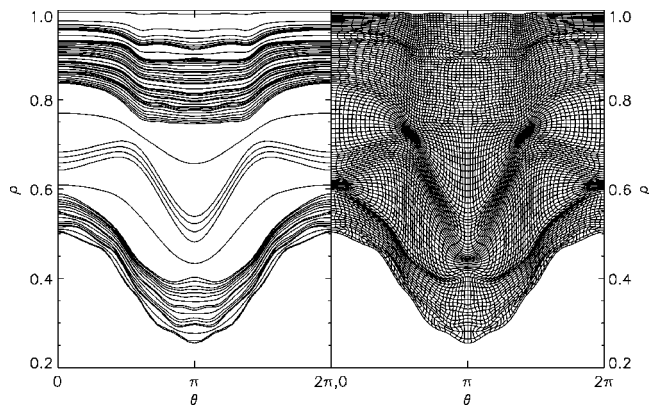


FIG. 4. (a) (left) A cross section of quadratic-flux minimizing surfaces chosen for radial framework, on the toroidal plane $\phi=0$. (b) (right) The resulting coordinate grid.

field shown in the constructed coordinate grid, where the field line tracings have been chosen to show the major island chains. Estimates for the island widths as calculated using Eq. (23) are shown by the solid horizontal lines. We can see from this graph that the $(n,m)=(2,1),(3,1)$ island chains form exactly where $q=2$ and 3 respectively for the constructed integrable field. For the $q=2$ islands, the half-widths of the islands closer to the radial location of q_{\min} , s_{\min} , are actually larger than the half-widths of the islands opposite s_{\min} . This is because near $s=s_{\min}$ the shear becomes small. In this case, it is a poor approximation to assume the shear is constant across the island region. Further improvement of the island estimates could be made by including the complete spectrum of perturbation terms in Eq. (23), rather than just the lowest order terms as done here.

The second example is demonstrated using a different selection of rational quadratic-flux minimizing surfaces. A different selection of rational quadratic-flux minimizing surfaces creates a different nearby integrable field. In fact, an integrable field that coincides with the actual nonintegrable field in regions of good flux surfaces is possible by choosing higher order rational surfaces. The drawback mentioned in the introduction, that such coordinates become singular at the separatrix, is demonstrated by the following. The quadratic-flux minimizing surfaces which will serve as the framework of the new radial coordinate are chosen with rational rotational-transforms approaching $q=2$ and 3 . These surfaces are shown in Fig. 4(a). The orders of the surfaces chosen, in increasing radial location, are (11,26), (14,33), (3,7), (13,30), (10,23), (7,16), (11,25), (4,9), (13,29), (9,20), (5,11), (11,24), (6,13), (13,28), (7,15), (8,17), (9,19), (1,2), (12,23), (11,21), (11,21), (12,23), (1,2), (13,28), (6,13), (11,24), (5,11), (9,20), (4,9), (11,25), (7,16), (10,23), (13,30), (3,7), (11,26), (8,19), (5,12), (7,17), (9,22), (11,27), (2,5), (9,23), (7,18), (5,13), (8,21), (3,8), (10,27), (7,19), (4,11), (5,14), (6,17), (7,20), (8,23), (9,26), (10,29), (1,3), (8,25), (7,22), (6,19), (5,16), (4,13), (3,10), (2,7), and (1,4). The surfaces with large denominators typically coincide with flux surfaces of the given nonintegrable field. This is observed via the action gradients of the surfaces becoming very small. The associated coordinate grid is shown in Fig. 4(b). The coordi-

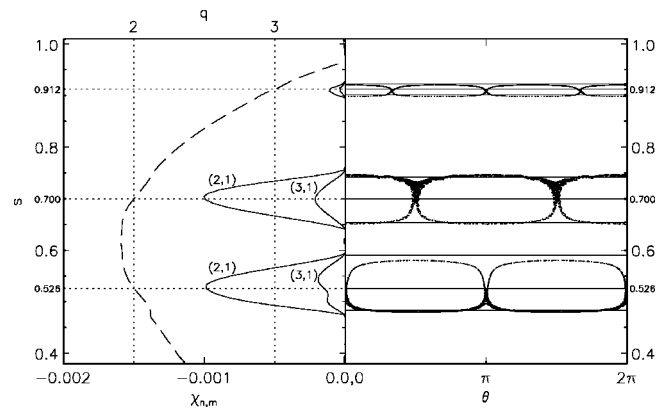


FIG. 5. (a) (left) Resonant perturbations with $(n,m)=(2,1),(3,1)$ shown with solid lines, and the q profile shown with dashed line. (b) (right) The Poincaré plot in new coordinates showing $(n,m)=(2,1),(3,1)$ island chains with the $(2,1)$ and $(3,1)$ rational surfaces and estimated island widths plotted as solid lines on the right. Coordinates correspond to those shown in Fig. 4.

nates, though still smooth, are approaching singularity. The singularity in the coordinates can be observed in the radial dependence of the perturbation harmonics $\chi_{2,1}$ and $\chi_{3,1}$, which are shown in Fig. 5(a). As the surfaces chosen for the coordinate radial function approach the separatrix, the radial region where the perturbation function is nonzero reduces in width. By using quadratic-flux minimizing surfaces that lie just outside the separatrices of the $(2,1)$ and $(3,1)$ islands, the $(2,1)$ and $(3,1)$ islands become square when plotted in the constructed coordinates as is shown in Fig. 5(b). Note that for this case, as the perturbation terms become more peaked, the estimate for the island width becomes less accurate.

VI. DISCUSSION

The choice of rational rotational-transform quadratic-flux minimizing surfaces has a great impact on the structure of the constructed integrable field. Surfaces may be chosen to focus attention on specific features of the given nonintegrable field, or to avoid regions which are not relevant to the particular application. In addition to the features already displayed in the previous section, some additional applications may be mentioned.

We may approximate the separatrix of a low-order island chain by constructing quadratic-flux minimizing surfaces with rotational-transforms that approach the rationality of the low-order island chain. For example, the surfaces with rationalities corresponding to $(n,m)=(35,17),(37,18),(39,19),(41,20),\dots$ will lie just outside the separatrix of the $(n,m)=(2,1)$ island chain to one side, and the surfaces with $(n,m)=(35,18),(37,19),(39,20),(41,21),\dots$ will lie just outside the separatrix to the other. Surfaces may be chosen that automatically locate the regions outside major separatrices, and thus the regions of the nonintegrable field for which, to a good approximation, straight-field-line coordinates may be constructed.

KAM surfaces of the nonintegrable field may be approximated by constructing quadratic-flux minimizing sur-

faces with rotational transforms that approach certain irrationals, in particular the noble irrationals. By locating the KAM surfaces, we may construct coordinates that neatly compartmentalize regions of chaos. Also, by constructing a sequence of quadratic-flux minimizing surfaces with rotational-transforms approaching certain irrationals, we obtain a method by which the existence of KAM surfaces may be predicted. The action-gradient parameter determined during the construction of each quadratic-flux minimizing surface is directly related to the resonant perturbation harmonic amplitude and thus the island width.¹⁰ By estimating the degree of island overlap for high-order island chains adjacent to irrational surfaces, we may determine whether the associated KAM surface exists, or whether overlapping island chains have produced chaos in that region of space.¹⁷

The dominant computational expense of this construction is in the magnetic field line tracing. This cost is determined partly by the accuracy of the Fourier representations required. In this calculation, about 200 to 300 toroidal transits were required to locate a family of periodic pseudo-orbits and thus describe each surface. By exploiting the periodicity of the field lines, high-order rational rotational-transform surfaces require approximately the same amount of magnetic field line tracing as low-order rational rotational-transform surfaces.¹⁸ This number of transits provides the accuracy required for the purpose of demonstration, but for general applications, where less accuracy may suffice, fewer toroidal transits will be required.

VII. CONCLUSION

We have demonstrated a computationally efficient, theoretically insightful, and natural method of understanding nearly integrable magnetic fields and constructing flux coordinates. A nearby integrable field is constructed which minimizes the quadratic-flux functional on rational surfaces and the Fourier terms of the perturbation from integrability are determined. The estimates for the island widths provided by

the shear and perturbation harmonic amplitudes agree very well with detailed Poincaré plots. The flexibility of the approach has been demonstrated by constructing a nearby integrable magnetic field which closely coincides with the original magnetic field in regions where the island content is low. The present algorithm may be combined with other algorithms to locate rational flux surfaces, to quickly estimate island widths, to reliably locate high-order flux surfaces adjacent to low-order islands of significant width, and to locate the periodic X and O points of island chains.

ACKNOWLEDGMENTS

The authors are very grateful to Dr. D.A. Monticello for the use of the PIES code and various discussions. One of the authors (S. R. H.) would like to thank the staff at the Plasma Theory Laboratory at JAERI, and the support of a Science and Technology Agency (STA) of Japan postdoctoral fellowship.

¹A. J. Lichtenberg and M. A. Leiberman, *Regular and Chaotic Dynamics*, 2nd ed. (Springer, New York, 1992).

²H. Goldstein, *Classical Mechanics*, 2nd ed. (Addison-Wesley, Massachusetts, 1980).

³J. R. Cary and R. G. Littlejohn, *Ann. Phys.* **151**, 1–34 (1983).

⁴A. H. Boozer, *Phys. Fluids* **24**, 1999 (1981).

⁵A. Reiman and N. Pomphrey, *J. Comput. Phys.* **94**, 225 (1991).

⁶A. H. Boozer, *Phys. Fluids* **26**, 1288 (1983).

⁷M. Kaasalainen and J. Binney, *Phys. Rev. Lett.* **73**, 2377 (1994).

⁸A. H. Reiman and H.S. Greenside, *J. Comput. Phys.* **87**, 349 (1990).

⁹R. L. Dewar, S. R. Hudson, and P. Price, *Phys. Lett. A* **194**, 49 (1994).

¹⁰S. R. Hudson and R. L. Dewar, *Phys. Lett. A* **247**, 246 (1998).

¹¹W. D. D'haeseleer, W. N. G. Hitchon, J. D. Callen, and J. L. Shohet, *Flux Coordinates and Magnetic Field Structure* (Springer, Berlin, 1991).

¹²D. K. Arrowsmith and C. M. Place, *An Introduction to Dynamical Systems* (Cambridge University Press, Cambridge, 1991).

¹³S. R. Hudson and R. L. Dewar, *Phys. Lett. A* **226**, 85 (1997).

¹⁴A. H. Reiman and H. S. Greenside, *Comput. Phys. Commun.* **43**, 157 (1986).

¹⁵H. Shirai and JT-60 team, *Phys. Plasmas* **5**, 1712 (1998).

¹⁶S. Ishida and JT-60 team, *Phys. Rev. Lett.* **79**, 3917 (1997).

¹⁷S. R. Hudson, Ph.D. thesis, Australian National University, 1997.

¹⁸S. R. Hudson and R. L. Dewar, *J. Plasma Phys.* **56**, 361 (1996).